Volume 17, Number 1, 2024. pp. 125-134

Jordan Journal of Physics

ARTICLE

Temperature Dependent Behavior of Elastic and Ultrasonic Proprieties of Transition Metal Carbide Mo_2C Superconductor

Sachin Rai and **Pramod K. Yadawa**

Department of Physics, Prof. Rajendra Singh (Rajju Bhaiya) Institute of Physical Sciences for Study and Research, V. B. S. Purvanchal University, Jaunpur - 222003, India.

Doi: **https://doi.org/10.47011/17.1.12**

Received on: 19/07/2022; *Accepted on: 15/09/2022*

Abstract: Transition metal carbides exhibit peculiar chemical and physical properties, making them integral to industrial applications that demand performance under high temperatures In the case of the hexagonal transition metal carbide Mo_2C superconductor, higher-order elastic constants were calculated to be temperature-dependent using an interactional potential model. Second-order elastic constants are used to determine other allied ultrasonic variables. Second-order coefficients are used to analyze the temperature variation of ultrasonic velocities along the z-direction of the superconductor. Furthermore, the temperature difference of Debye average velocity and thermal relaxation time are considered along the same direction. The temperature dependence of ultrasonic properties is explored in relation to thermal, elastic, and mechanical properties. Ultrasonic attenuation , resulting from phonon–phonon (p–p) interactions, is calculated at different temperatures .The study establishes that thermal conductivity is a core provider of the observed ultrasonic attenuation, particularly at higher temperatures. The mechanical and thermal properties of the Mo_2C superconductor are superior at lower temperatures.

Keywords: Transition metal carbide superconductor, Thermal conductivity, Ultrasonic properties, Elastic properties, Mechanical properties.

PACS numbers: 43. 35. Cg; 62.20.Dc; 63.20.Kr.

Introduction

Transition metal carbides (TMCs) are garnering attention owing to significant chemical and physical properties, including enhanced chemical stability, maximum hardness, high melting points,excellent thermal conductivity, and outstanding corrosion and wear resistance. These unique properties make them highly desirable for various applications, particularly in cutting equipment and wear-resistant components that operate under high temperatures and pressures [1]. Mo_2C shows great potential for use in microelectronics as diffusion barriers and electrical connections [2, 3]. TMCs have played a main role in advancing structural steels, contributing to the strengthening and toughening of micro alloyed steels, as well as the development of heat-resistant steels[4]. Mo_2C superconductors have a hexagonal closed-packed structure with a space group $P6_3/mmc$ and crystal constants of a = 0.3015 nm, b = 0.3015 nm, and c = 0.4786 nm [5, 6]. Recent research has also explored the potential of TMCs in the field of two-dimensional superconductivity [7-9]. Mo_2C superconductors exhibit a Tc of 2.78K, attracting significant interest in various research endeavors[10, 11]. Furthermore, studies have highlighted the role of transition metal carbide in promotingthe polarization of supported metallic particles[12-14]. The hexagonal phase of Mo_2C

Corresponding Author: Sachin Rai **Email**: drsrphyjrf@gmail.com

is well known for its excellent catalytic activity in a wide variety of reactions, such as hydrogenation of benzene [15], hydrogenation of alkanes [16], and alkane isomerization.

Ultrasonic attenuation (UA) is a crucial physical parameter that accurately characterizes the behavior ofa substance, reflecting specific interactions between the anisotropic nature of proximal hematinic planes and structural motion.It is linked to various physical processes, such as specific heat, thermal conductivity, thermal energy density, and higher-order elastic coefficients [17].

In this work, we aimed to establish a correlation between the thermo-physical and microstructural characteristics of hexagonal Mo_2C superconductors. This relationship will help us understand the mechanical behavior of transition metal carbides and can provide valuable insights for optimizing manufacturing processes under proper conditions. We have measured the ultrasonic attenuation coefficient, acoustic coupling constants, elastic stiffness coefficients, thermal relaxation time, and ultrasonic velocities for the Mo_2C superconductor. Shear modulus (G), bulk modulus (B), Young's modulus (Y), Pugh's ratio (B / G), Poisson's ratio, and anisotropic index were also considered and discussed in the context of Mo_2C superconductors.

Theory

There are numerous approaches to analyzing high-order (SOECs, TOECs) elastic factors of hexagonal materials. In our current effort, we utilized the Lenard-Jones interaction potential approach for the evaluation of SOECs and TOECs.

A common description of n^{th}-order elastic constant is the partial derivatives of the thermodynamic potential of the medium-constrained finite deformation, mathematically conveyed by the subsequent expression [18, 19]:

$$C_{ijklmn\ldots} = \frac{\partial^n F}{\partial\eta_{ij}\partial\eta_{kl}\partial\eta_{mn}\ldots.} \quad (1)$$

Here, F denotes free energy density and η_{ij}represents the Lagrangian strain component tensor. Fcan be expanded in terms of strain η by the Taylor series expansion:

$$F = \sum_{n=0}^{\infty} F_n = \sum_{n=0}^{\infty} \frac{1}{n!}\left(\frac{\partial^n F}{\partial\eta_{ij}\partial\eta_{kl}\partial\eta_{mn\ldots}}\right)\eta_{ij}\eta_{kl}\eta_{mn}\ldots \quad (2)$$

Thereby, the free energy density is written as:

$$F_2 + F_3 = \frac{1}{2!}C_{ijkl}\eta_{ij}\eta_{kl} + \frac{1}{3!}C_{ijklmn}\eta_{ij}\eta_{kl}\eta_{\mathrm{mn}} \quad (3)$$

In hexagonal compounds, the basic vectors are $a_1 = a\left(\frac{\sqrt{3}}{2}, \frac{1}{2}, 0\right)$, $a_2 = a(0,1,0)$, and $a_3 = a(0,0,c)$in Cartesian coordinates axis. Here,a and c are the unit cell lattice parameters. The unit cell of an HCP compound contains two nonequivalent atoms: 6 atoms in the basal plane and 3 atoms above and below the basal plane. Consequently, both the first and second neighborhoods contain 6 atoms. The location vectors of these two kinds of atoms are$r_1 = a(0,0,0)$and $r_2 = \left(\frac{a}{2\sqrt{3}}, \frac{a}{2}, \frac{c}{2}\right)$.

The potential energy per unit cell up to the second adjacent neighbor is described as:

$$U_2 + U_3 = \Sigma_{I=1}^{6} \quad U(r_I) + \Sigma_{J=1}^{6} \quad U(r_J) \quad (4)$$

Here, I refers to atoms in the basal plane and J refers to atoms above and below the basal plane. When the crystal is uniformlydeformable, the interatomic vectors in thenon-deformed state (r) and the deformable state (r') are associated as:

$$(r')^2 - (r)^2 = 2\varepsilon_i\varepsilon_j\eta_{ij} = 2\Theta \quad (5)$$

whereε_i and $\varepsilon_j$are the Cartesian components of vector r. The energy density Ucan be describedbased onΘas [27, 28]:

$$U_n = (2V_c)^{-1}\Sigma\frac{1}{n!}\Theta^n D^n\varphi(r) \quad (6a)$$

Based on Eqs. (4) and (6), the energy density U involving cubic terms can be written as:

$$U_2 + U_3 = (2V_c)^{-1}\left[\sum_{I=1}^{6}\frac{1}{2!}{\Theta_I}^2 D^2\varphi(r_I) + \sum_{J=1}^{6}\frac{1}{2!}{\Theta_J}^2 D^2\varphi(r_J)\right] + (2V_c)^{-1}\left[\sum_{I=1}^{6}\frac{1}{3!}{\Theta_I}^3 D^3\varphi(r_I) + \sum_{J=1}^{6}\frac{1}{3!}{\Theta_J}^3 D^3\varphi(r_J)\right] \quad (6b)$$

Here, $V_c = [3^{1/2}/2]\, a^2 c$ signifies the volume of the elementary cell, $D=R^{-1}d/dR$, and $\varphi(r)$is the interaction potential. The energy density is examined to be a function of the Lennard-Jones

potential and specified as:

$$\varphi(r) = -\frac{a_0}{r^m} + \frac{b_0}{r^n} \tag{7}$$

where, a_0, b_0 are constants; m, n are the integers and 'r' is the distance between atoms. To establish the interaction potential model leading to the computation of six SOECs and ten TOECs of the hexagonal compound, the formulations of elastic constants are given by the following expressions [18, 19]:

$$\left.\begin{aligned} C_{11} &= 24.1\mathrm{p}^4C'C_{12} = 5.918\mathrm{p}^4C' \\ C_{13} &= 1.925\mathrm{p}^6C'C_{33} = 3.464\mathrm{p}^8C' \\ C_{44} &= 2.309p^4C'C_{66} = 9.851\mathrm{p}^4C' \end{aligned}\right\} \tag{8a}$$

$$\left.\begin{aligned} C_{111} &= 126.9p^2B + 8.853p^4C'C_{112} \\ &= 19.168p^2B - 1.61p^4C' \\ C_{113} &= 1.924p^4B + 1.155p^6C'C_{123} \\ &= 1.617p^4B - 1.155p^6C' \\ C_{133} &= 3.695p^6BC_{155} = 1.539p^4B \\ C_{144} &= 2.309p^4BC_{344} = 3.464p^6B \\ C_{222} &= 101.039p^2B + 9.007p^4C'C_{333} \\ &= 5.196p^8B \end{aligned}\right\} \tag{8b}$$

where p = c/a: axial ratio;$C' = \chi\ \mathrm{a}\ /\ \mathrm{p}^5$; $B = \psi \mathrm{a}^3/p^3$;$\chi = (1/8)[\{nb_0\ (n-m)\}/\{\mathrm{a}^{n+4}\}]\psi = -\chi\ /\{6\ \mathrm{a}^2(m+n+6)\}$; m, n=integer quantity, and b_0=Lennard-Jones parameter.

The bulk modulus and shear modulus were calculated using Voigt and Reuss' methodologies [20, 21]. The calculations of unvarying stress and unvarying strain were used in the Voigt and Reuss' methodologies, correspondingly. Furthermore, from Hill's methods, the average values of both methodologies were used to compute the ensuing values of B and G [22]. Young's modulus and Poisson's ratio are considered using values of bulk modulus and shear modulus, respectively [23, 24]. The following expressions were used for the evaluation of Y, B, G, and σ.

$$\left.\begin{aligned} M &= C_{11} + C_{12} + 2C_{33} - 4C_{13};\ \mathrm{C}^2 \\ &= (C_{11} + C_{12})C_{33} - 4C_{13} + C^2{}_{13}; \\ B_R &= \frac{C^2}{M};\ \mathrm{B}_V = \frac{2(C_{11}+C_{12})+4C_{13}+C_{33}}{9}; \\ G_V &= \frac{M+12(C_{44}+C_{66})}{30}; \\ \mathrm{G}_R &= \frac{5C^2C_{44}C_{66}}{2[3B_VC_{44}C_{66}+C^2(C_{44}+C_{66})]}; \\ Y &= \frac{9GB}{G+3B};\ \mathrm{B} = \frac{B_V+B_R}{2}; \\ \mathrm{G} &= \frac{G_V+G_R}{2};\ \sigma = \frac{3\mathrm{B}-2\mathrm{G}}{2(3\mathrm{B}+G)} \end{aligned}\right\} \tag{9}$$

The anisotropic and mechanical properties of nanostructured materials are well correlated with ultrasonic velocity, as the velocity of ultrasonic waves mainly depends on the SOECs and density. Depending on the mode of vibration, there are three types of ultrasonic velocities in hexagonal nanostructured compounds: longitudinal (V_L)and two shear waves (V_{S1}, V_{S2}). The ultrasonic velocities based on the angle between the direction of propagation and the z-axis for hexagonal nanostructured compounds are given by the subsequent set of equations:

$$\left.\begin{aligned} V_L^2 &= \{C_{33}\,cos^2\,\theta + C_{11}\,sin^2\,\theta + C_{44} \\ &\quad +\{[C_{11}\,sin^2\,\theta - C_{33}\,cos^2\,\theta \\ &\quad +C_{44}(cos^2\,\theta - sin^2\,\theta)]^2 \\ &\quad +4\,cos^2\,\theta\,sin^2\,\theta\,(C_{13}+C_{44})^2\}^{1/2}\}/2\rho \\ V_{S1}^2 &= \{C_{33}\,cos^2\,\theta + C_{11}\,sin^2\,\theta \\ &\quad +C_{44} - \{[C_{11}\,sin^2\,\theta - C_{33}\,cos^2\,\theta \\ &\quad +C_{44}(cos^2\,\theta - sin^2\,\theta)]^2 \\ &\quad +4\,cos^2\,\theta\,sin^2\,\theta\,(C_{13}+C_{44})^2\}^{1/2}\}/2\rho \\ V_{S2}^2 &= \{C_{44}\,cos^2\,\theta + C_{66}\,sin^2\,\theta\}/\rho \end{aligned}\right\} \tag{10}$$

where, V_L, V_{S1}, and V_{S2} are the longitudinal, quasi-shear, and shear wave velocities. Also, 'ρ'is the density of the compound and θ is an angle with the unique axis of the crystal. For hexagonal nanostructured crystal, the Debye average velocity is specified by the equation as [25, 26]:

$$V_D = \left[\frac{1}{3}\left(\frac{1}{V_L^3} + \frac{1}{V_{s1}^3} + \frac{1}{V_{32}^3}\right)\right]^{-1/3} \tag{11}$$

The mathematical formulation of ultrasonic attenuation for longitudinal $(A)_{Long}$ and shear waves $(A)_{Shear}$ induced by the energy loss due to electron-phonon interaction is given by [26, 27]:

$$A_{long} = \frac{2\pi^2f^2}{\rho V_l^3}\left(\frac{4}{3}\eta_e + \chi\right) \tag{12}$$

$$A_{shear} = \frac{2\pi^2f^2}{\rho V_S^3}\eta_e \tag{13}$$

where 'ρ' is the density of the nanostructured compound, 'f' is the frequency of the ultrasonic wave, 'η_e' is the electron viscosity, and 'χ' is the compressional viscosity (which is zero in the present case), V_L and V_S are the acoustic wave velocities for longitudinal and shear waves, respectively, and are given as:

$$V_L = \sqrt{\frac{C_{33}}{\rho}}\text{and}\ V_S = \sqrt{\frac{C_{44}}{\rho}} \tag{14}$$

The viscosity of the electron gas (η_e) [25, 26] is given by:

$$\eta_e = \frac{9\times10^{11}h^2(3\pi^2N)^{2/3}}{5e^2R} \quad (15)$$

where 'N' represents the number of molecules per unit volume and 'R' is the resistivity.

At higher temperatures, p-p interaction (Akhieserloss) and thermo-elastic loss are the two prevailing processes, both of which contribute significantly to the attenuation of ultrasonic waves. The attenuation due to Akhieser loss is specified by the subsequent equation:

$$(A/f^2)_{Akh} = \frac{4\pi^2\tau E_0(D/3)}{2\rho V^3} \quad (16)$$

Here, f represents the frequency of the ultrasonic wave and E_0 is the thermal energy density. The measure of transforming acoustical energy into thermal energy is recognized as acoustical coupling constants, signified by D, and is specified by the subsequent expression:

$$D = 3(3E_0 < (\gamma_i^j)^2 > - < \gamma_i^j >^2 C_V T)/E_0 \quad (17)$$

where C_V is the specific heat capacity at the constant volume of the material, T is the temperature, and γ_i^j is the Grüneisen number, while i and j are the mode and direction of the propagation. While the ultrasonic waves transmit through the material, the equilibrium of lattice phonon distribution gets disturbed. The time taken for the re-establishment of equilibrium of the thermal phonons, known as the thermal relaxation time τ, is given by [26, 27]:

$$\tau = \tau_S = \tau_L/2 = \frac{3k}{C_V V_D^2} \quad (18)$$

where the thermal relaxation time for the longitudinal wave and shear wave are signified by τ_L and τ_S, correspondingly, and k is the thermal conductivity of the nanostructured compound. The thermoelastic loss $(\alpha/f^2)_{Th}$ is described by the equation:

$$(A/f^2)_{Th} = 4\pi^2 < \gamma_i^j >^2 \frac{kT}{2\rho V_L^5} \quad (19)$$

The total attenuation is specified by the subsequent equation as:

$$(A/f^2)_{Total} = (A/f^2)_{Th} + (A/f^2)_L + (A/f^2)_S \quad (20)$$

where $(A/f^2)_{Th}$ is the thermoelastic loss, while $(A/f^2)_L$ and $(A/f^2)_S$ are the ultrasonic attenuation coefficients for the longitudinal wave and shear wave, correspondingly.

Results and Discussions

Higher Order Elastic Constants

In the current investigation, we have calculated the elastic coefficients (6 SOECs and 10TOECs) using an interaction potential approach. The lattice parameters 'a' (basal plane parameter) and 'p' (axial ratio) for the Mo_2C superconductor are 3.015Å and 1.59, correspondingly [5, 6, 28]. The chosen values of m and n are 6 and 7 for the Mo_2C superconductor. The value of b_0 is taken at $2.26\text{x}10^{-64}$ erg cm^7 for the Mo_2C superconductor. Table 1 shows the values of the second and third-order elastic coefficients of the transition metal carbide.

TABLE 1.SOECs and TOECs (in GPa) of Mo_2C at room temperature.

SOEC→ Compounds↓	C_{11}	C_{12}	C_{13}	C_{33}	C_{44}	C_{66}
Mo_2C(Present)	482.9	118.6	97.5	443.6	116.9	189.4
Mo_2C [29]	480			448	169	150

TOEC→	C_{111}	C_{112}	C_{113}	C_{123}	C_{133}	C_{344}	C_{144}	C_{155}	C_{222}	C_{333}
Mo_2C	-7875	-1249	-250	-318	-1499	-1405	-370	-247	-6231	-5327

The maximum elastic constant parameters obtained for the Mo_2C superconductor are significant for the substance because they are connected to the stiffness constraint. SOECs are used to establish the ultrasonic attenuation and allied parameters. The highest elastic coefficient values established for transition-metal carbide Mo_2C are indicative of their improved mechanical properties.

For hexagonal structure material stability, the five different SOECs (C_{ij}, namely C_{11}, C_{12}, C_{13}, C_{33}, C_{44}) satisfy Born-Huang's norms [24, 25], which makes complete sense in view of Table 1. This superconductor is mechanically stable

because it is clear that the positive elastic constant values satisfy Born-mechanical Huang's stability constraints. The calculated values of C_{44} and C_{66} vary slightly from other theoretical results for Mo_2C compounds, where the evaluation was done using DFT [29], although the magnitude of SOECs C_{11}, C_{12}, C_{13}, and C_{33} are the same as given in Table 1 [29]. Thus, there is good agreement between the presented and given values. As a result, the theoretical approach for calculating SOECs of hexagonally structured superconductors at room temperature is well justified. Table1 illustrates the evaluated TOEC values. TOECs with negative values indicate strain within the solid. This aligns with previous findings on hexagonal-structured materials, affirming the theoretical framework's accuracy in valuing higher-order elastic coefficients. As a result, the theory used to investigate higher-order elastic coefficients is justified [30, 31]. Using Eq. (9), the values of bulk modulus (B), shear modulus (G), Young's modulus (Y), Pugh's ratio (B/G), toughness (G/B), and poison ratio (σ) for Mo_2C transition metal carbide at room temperature are determined and are shown in Table 2.

TABLE 2. Voigt–Reus' constants (M and C^2), B (x $10^{10}Nm^{-2}$), G (x $10^{10}Nm^{-2}$), Y (x $10^{10}Nm^{-2}$), σ, and B/G for Mo_2C superconductor transition metal carbide.

	M	C^2	B_r	B_v	G_r	G_v	Y	B/G	G/B	σ
Mo_2C	1098	276500	239	227	153	159	285	1.53	0.65	0.231

The values of B, Y, and G for Mo_2C transition metal carbide are observed to be smaller compared to other transition metal carbides. This indicates that Mo_2C has relatively lower stiffness and bonding strength. The ratios B/G and σ provide insights into the material's brittleness and ductility. Materials with $\sigma=0.23\leq0.26$ and $B/G = 1.52\leq1.75$ are typically considered brittle, or else they are ductile in nature [32, 33]. The fact that our results for B/G are lower than their critical values indicates that transition metal carbides are brittle at room temperature. The value of σ which should ideally be less than 0.5 for elastic and stable materials, is found to be within an acceptable range for Mo_2C.

It is clearly seen that the Mo_2C superconductor is dependable under shear. The higher hardness results from a higher degree of covalent bonding. The material's mechanical properties, such as ductility, stiffness, toughness, brittleness, and bonding properties, are closely connected to the second-order elastic coefficients. To quantify the degree of anisotropy in the material, various anisotropic indexes are employed. In the present work, the general anisotropic index (A^U) and percent anisotropy (A_S and A_G) have been calculated [34]. The values of the anisotropic index and percent anisotropy for Mo_2C transition metal carbide are 0.095, 0.052, and 0.019,respectively. An anisotropic index of zero indicates an isotropic structure, whereas non-zero values denote anisotropic constitution.A^U is a superior indicator for mechanical anisotropic properties, with higher values indicating stronger anisotropy of the compound.

Ultrasonic Velocity and Allied Constraints

The elastic modulus and isotropic properties of the material were correlated through ultrasonic velocity in the current analysis. For Mo_2C transition-metal carbide, we have determined the Debye average velocity (V_D), longitudinal velocity (V_L), shear velocity (V_S), and relaxation time (τ). The data used for the Mo_2C superconductor's temperature-dependent density (ρ) are shown in Table 3 and were obtained from the existing literature [28]. The Mo_2C transition-metal carbide thermal conductivity (k), shown in Table 3, was obtained from the literature [28]. Additionally, the thermal conductivity of superconductor Mo_2C has been evaluated using electrical resistivity via the Wiedemann-Franz law [30]. Debye temperatures (Θ_D), acoustic coupling coefficients (D_L and D_S), specific heat per unit volume (C_V), and the thermal energy density (E_0) as a function of temperatures are shown in Table3**,** According to the table of physical constants.

TABLE 3. Density (ρ: in 10^3 kg m^{-3}), specific heat capacity at constant volume (C_V: in $10^5 Jm^{-3}K^{-1}$), thermal energy density (E_0: in $10^7 Jm^{-3}$), thermal conductivity (k: in$10^{-2} Wm^{-1}K^{-1}$), and acoustic coupling constant (D_L, D_S) of Mo_2C superconductor.

	ρ	C_V	E_0	k	D_L	D_S
50K	9.00	1.11	0.15	6.28	53.29	1.30
100K	8.98	4.75	1.61	7.68	54.35	1.30
150K	8.96	7.23	4.62	8.08	55.22	1.30
200K	8.94	8.47	8.69	8.55	55.79	1.30
250K	8.92	9.33	13.09	9.02	56.02	1.30
300K	8.90	9.77	17.87	9.22	56.23	1.30

Table 3 shows clearly that for transition metal carbides, the values of D_L are often greater than those of D_S. It has been shown that less ultrasonic energy is converted into thermal energy for shear ultrasonic waves than for longitudinal ultrasonic waves.

Figs. 1-4 show the angular correlations of ultrasonic velocities (V_L, Vs_1, V_{S2}, V_D) at various temperatures along the z-axis of the superconductor. In Figs. 1 and 2, the z-axis of the superconductor correlates directly to the minima and maxima of the ultrasonic velocities V_L and V_{S1} of the Mo_2C superconductor. In Fig. 3, V_{S2} rises through the angle away along the z-direction. The combined effects of SOECs and ρ (density) are held responsible in favor of the uncharacteristic behavior of angle-dependent velocity. The existence of the angle (Θ) - dependent velocity (V) curves in this effort is comparable to that discovered for other hexagonal-type materials [31-33]. Thus, the angle dependence of the velocities in transition metal carbide is justified.

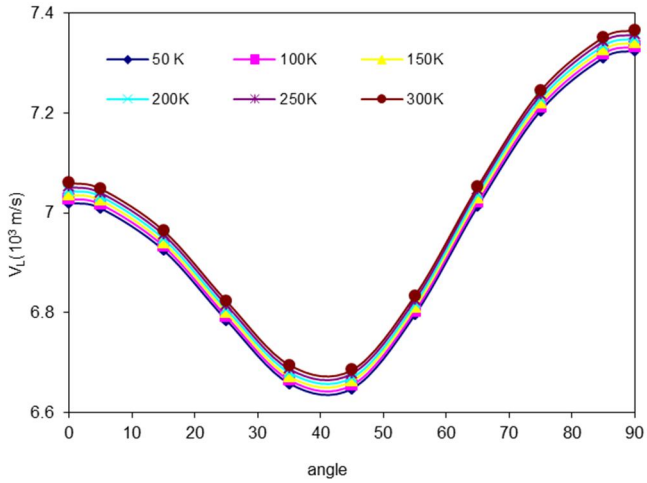

FIG. 1. V_L vs. angle (Θ) with z- axis of Mo_2C.

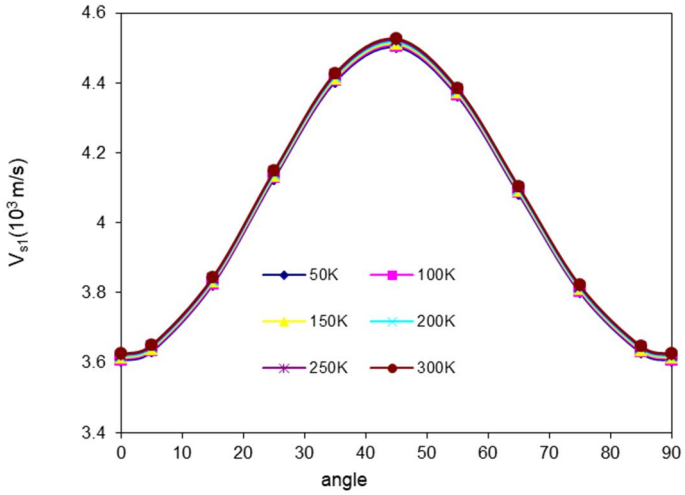

FIG. 2. V_{S1} vs. angle with z- axis of Mo_2C.

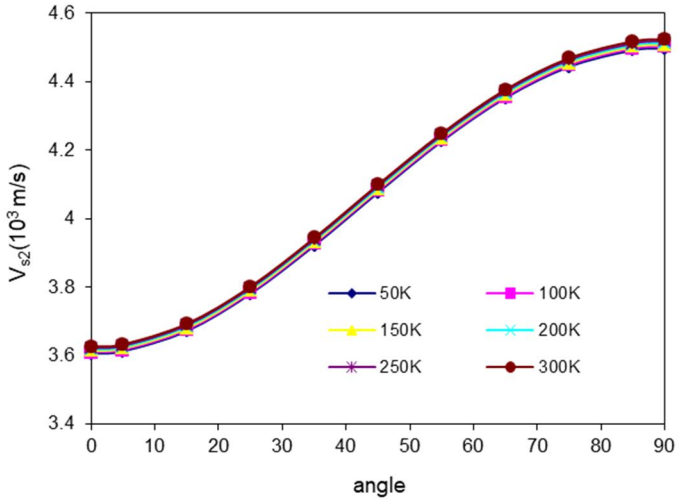

FIG. 3. V_{S2} vs. angle with z- axis of Mo_2C.

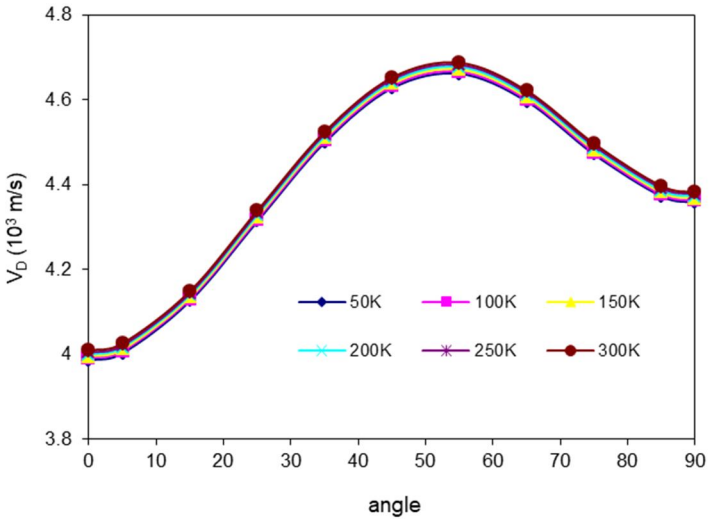

FIG. 4. V_D vs. angle (Θ) with z- direction of Mo_2C.

Fig. 4 illustrates the relationship between the average Debye velocity (V_D) and the (Θ) angle formed through the crystal z-direction. The transition metal carbide Mo_2C superconductor's V_D clearly increases with Θ (angle) and reaches its limit at 55^0 because the fundamental ultrasonic velocities V_L, V_{S1}, and V_{S2} are used in the calculation of V_D [34, 35], so it is reasonable that the variation of V_D (Debye average velocity) is influenced through these velocities. The limit of V_D at 55 ° is caused by an increase in V_L and V_S, as well as a decrease in quasi-shear wave velocity. The common sound wave velocity is the greatest when a sound wave moves by 55^0 degrees by these crystals' z-axis

The evaluated value of thermal relaxation time 'τ' correlated with the angle is plotted in Fig. 5. The reciprocal character of V_D as $\tau \propto 3k/C_V V_D^2$ is tracked by angle (Θ)-dependent thermal relaxation time (τ) curves. It is evident that thermal conductivity exerts the most significant influence on the thermal relaxation time of the transition metal carbide superconductor. These results indicate that 'τ' falls within the picosecond range for hexagonally shaped substances [36, 37]. Therefore, the hexagonal structure of the transition metal carbide can be elucidated by the calculated thermal relaxation time. Remarkably, the shortest re-establishment time required for the stability distribution of thermal phonons corresponds to wave propagation along $\tau = 55^0$, as indicated by the minimum value of 'τ'.

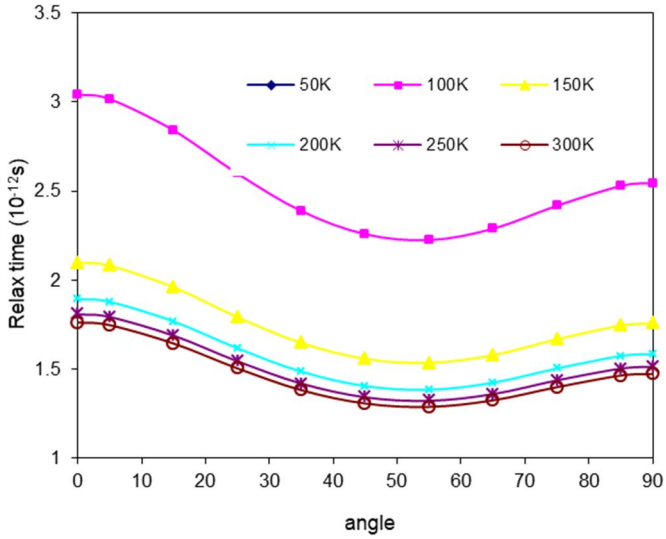

FIG. 5. Relaxation time (τ) vs angle (Θ) with z- axis of Mo_2C.

Ultrasonic Attenuation Due To P-P Interaction and Thermal Relaxation Occurrences

While calculating the ultrasonic attenuation (UA), it is assumed that the wave is propagated along the z-axis [<001> axis's] of Mo_2C transition-metal carbide. The attenuation constants of the longitudinal wave $(A/f^2)_L$ and the shear wave $(A/f^2)_S$are determined by Eq. (16) under the conditionωτ<<1at various temperatures.Figures6 and 7 show the values for the temperature-dependent $(A/f^2)_L$, $(A/f^2)_S$, $(A/f2)_{Th}$, and total attenuation $(A/f^2)_{total}$ of Mo_2C transition metal carbide. The thermoelastic loss divided by frequency squared $(A/f^2)_{Th}$ has been calculated using Eq. (19).

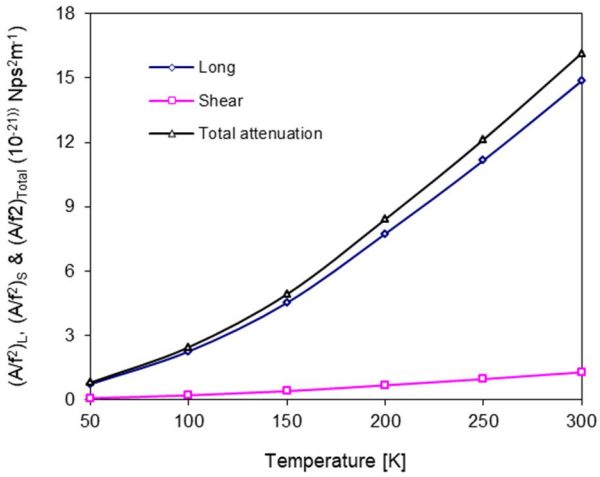

FIG. 6. $(A/f^2)_L$, $(A/f^2)_S$, $(A/f^2)_{Total}$ vs temperature of Mo_2C.

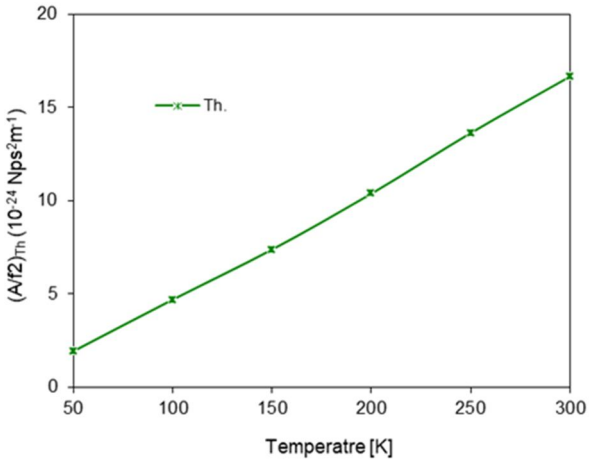

FIG. 7. $(A/f^2)_{Th}$ vs temperature of Mo_2C.

In this work, the ultrasonic wave (V) is assumed to propagate along the z-axis of the superconductor, as shown in Fig. 6. It is obvious that the Akhieser form of energy losses favors longitudinal waves, shear waves, and thermoelectric losses, all of which increase with the temperature of the compounds.$(A/f^2)_{Akh}$ is proportional to D, E_0, τ, and V^{-3}, as described by Eqs. (16) and (17). Figure 3 illustrates that' E_0, and'V'increase with high temperature, consequently impacting Akhieser losses in the Mo_2C superconductor through E_0 also the' k'.

Consequently, the increase in UA is due to the increase in thermal conductivity. Therefore, it is the p-p interaction that predominantly governs the ultrasonic attenuation. Owing to the lack of experimental data in the literature, an evaluation of ultrasonic attenuation could not be conducted.

From Fig. 7, it is obvious that the thermoelastic loss is significantly smaller than Akhieser loss for Mo_2C transition metal carbide, as well as the total attenuation. Ultrasonic attenuation due to p–p interaction for longitudinal wave and shear wave is the dominant factor. The thermal energy density and the thermal conductivity are the most important factors that affect the total attenuation. Consequently, it could be predicted that the transition metal carbide superconductor behaves as its purest variety at low temperatures and isthe mostductile, confirmed by the minimum attenuation. Although at room temperature, Mo_2C transition-metal carbide is the least ductile. Consequently, at low temperatures (50K), there would be the least impurity in the Mo_2C superconductor. The minimum UA for Mo_2C transition metal carbide least defends its quite stable hexagonally structured Mo_2C.

Conclusions

Based on the above discussion, the following conclusions are drawn:

- The standard calculation technique for higher-order elastic coefficients for hexagonal transition-metal carbide Mo_2C superconductors, based on a Lenard-Jones potential model, remains applicable.
- The elastic properties of Mo_2C superconductors imply that this transition metal carbide is mechanically stable.
- Young's moduli of Mo_2C transition metal carbide have more anisotropic structures than bulk modulus, as projected using numerous anisotropic indexes.
- The thermal relaxation time of Mo_2C transition metal carbide is established to order of picoseconds, defending its hexagonal structure. The smallest significance of 'τ' along = 55^0 at all temperatures indicates that the time required to re-establish the equilibrium distribution of phonons for wave propagation in this direction will be the shortest.
- Over total attenuation, UA caused by the p-p interaction mechanism is dominant and is a leading factor of thermal conductivity
- The mechanical properties of the Mo_2C transition-metal carbide are observed to be better at low temperatures (50K).
- Mo_2C superconductor exhibit their purest variety at low temperatures and demonstrate increased ductility, as verified by the minimum attenuation. However, at room temperature, transition-metal carbide is observed to be the least ductile.

This research could help in computational as well as non-destructive classification of transition-metal carbides. These findings serve as the basis for further research into the major thermo-physical properties of other transition-metal carbides.

Acknowledgments

Authors are thankful to Veer Bahadur Singh Purvanchal University (133/VBSPU/IQAC/ 2022, Date. 23-03-2022) minor project grant (Code: 50) and Council for Scientific and Industrial Research–University Grant Commission (CSIR–UGC) for providing financial assistance in form of CSIR - Junior Research Fellowship (1500/CSIR-UGC NET dec, 2017) India.

References

[1] Clinard, F.W., Kempter, J.R. and Kempter, C.P.J., Less Common Met., 15 (1968) 59.

[2] Martinelli, A.E., Drew, R.A.L. and Berriche, R., J. Mater. Sci. Lett., 15 (1996) 307.

[3] Lucazeau, E., Deneuville, A., Fontenille, J., Brunet, F. and Gheeraert E.,Diam. Relat. Mater., 5 (1996) 779.

[4] Yamasaki, S. and Bhadeshia, H.K.D.H., Mater. Sci.Technol., 19 (2003) 723.

[5] Parthe, E. and Sadagopan, V., Acta Crystallogr., 16 (1963) 202.

[6] Reddy, K.M., Rao, T.N., Revathi, J. and Joardar, J.,J. Alloy. Compd., 494 (2010) 386.

[7] Song, S., Wang, L., Xu, C., Cheng, H., Ren, W. and Kang, N., IEEE Trans. Magn., 53 (2017) 7100404.

[8] Cetinkaya, S. and Eroglu, S., JOM, 69 (2017) 1997.

[9] Chuan, X., Libin, W., Zhibo, L., Long, C., Jingkun, G., Ning, K., Xiu-Liang, M., Hui-Ming, C. and Wencai, R., Nat. Mater., 17 (2015) 1135.

[10] Meisnner, W. and Franz, H., "MessungenmitHilfe von Flussigen Helium IX",(Supraleitfahigkeit von Carbiden and Nitrogen, Zeitschrift fur Physik, 1930).

[11] Matthias, B.T. and J. Hulm, K., Phys. Rev., 87 (1952) 799.

[12] Florez, E., Gomez, T., Rodriguez J.A. and Illas, F., Phys. Chem. Chem. Phys., 136 (2011) 6865.

[13] Florez, E., Feria, L., Vines, F., Rodriguez, J.A. and Illas,F., J. Phys. Chem., C, 113 (2009) 19994.

[14] Gomez, T., Florez, E., Rodriguez, J.A. and Illas, F., J. Phys.Chem. C,115 (2011) 11666.

[15] Lee, J.S., Yeom, M.H., Park, K.Y., Nam, I-S., Chung, J.S. and Kim, Y.G., J. Catal., 128 (1991) 126.

[16] Ledoux, M.J., Pham-Huu, C., Dunlop, H.M.,and Guille,J., J. Catal., 134 (1992) 383.

[17] Yadawa, P.K., PramanaJ. Phys., 76 (4) (2011) 613.

[18] Rai, S., Chaurasiya, N.,and Yadawa, P.K., Phys. Chem. Solid State, 22 (2021) 687.

[19] Pandey, D.K., Yadawa, P.K. and Yadav, R.R., Mater. Lett., 61 (2007) 5194.

[20] Voigt, W., "Lehrbuch der kristallphysik", (mitausschluss der kristalloptik),(Leipzig Berlin, B.G. Teubner, 1928).

[21] Reuss, A.,J. Appl. Math. Mech., 9 (1929) 49.

[22] Hill, R., Proc. Phys. Soc. A., 65 (1952) 349.

[23] Turkdal N., Deligoz, E., Ozisik, H. and Ozisik, H.B., Ph. Transit., 90 (2017) 598.

[24] Weck, P.F., Kim, E., Tikare, V. and Mitchell, J.A., Dalton Trans., 44 (2015) 18769.

[25] Singh, D., Pandey, D.K., Yadawa, P.K. and Yadav, A.K., Cryogenics, 49 (2009) 12.

[26] Singh, S.P., Yadawa, P.K., Dhawan, P.K., Verma, A K. and Yadav,R.R., Cryogenics, 100 (2019) 105.

[27] Singh, D., Yadawa, P.K. and Sahu, S.K., Cryogenics, 50 (2010) 476.

[28] Lue, F., Jhu, X., Jhu, J. and Tian, M., J. Cryst. Growth, 517 (2019) 24.

[29] Connetable, D., Mater. Res. Express, 3 (2016) 126502.

[30] Yadawa, P.K., Arab. J. Sci. Eng., 37 (2012) 255.

[31] Yadawa,P.K., Adv. Mat. Lett., 2 (2011) 157.

[32] Yadav, N., Singh, S.P., Maddheshiya, A.K., Yadawa, P.K. and Yadav, R.R., Ph. Transit., 93 (2020) 883.

[33] Yadav, C.P., Pandey, D.K. and Singh, D., Indian J. Phys., 93 (2019) 1147.

[34] Feng, B.X., Wan, C.L., Qu, Z.X., Huang, Z.C., Chen, J.C., Zhou, R. and Pan, W., Acta Mater., 59 (2011) 1742.

[35] Jaiswal, A.K., Yadawa, P.K. and Yadav, R.R., Ultrasonics, 89 (2018) 22.

[36] Singh, S.P., Singh, G., Verma, A.K., Yadawa, P.K. and Yadav, R.R., PramanaJ. Phys., 93 (2019) 83 (1-9).

[37] Yadawa, P.K., Ceram.-Silik., 55 (2011) 127.